

## SUPPLEMENTARY INFORMATION

# Metal ion binding properties of a bimodal triazolyl-functionalized calix[4]arene on a multi-array microcantilever system. Synthesis, fluorescence and DFT computation studies

Author(s): Abdullah N. Alodhayb,<sup>a</sup> Mona Braim,<sup>a</sup> L.Y. Beaulieu<sup>a</sup>, Gopikishore Valluru,<sup>b</sup> Shofiur Rahman,<sup>b</sup> Ahmed K. Oraby<sup>b</sup> and Paris E. Georghiou<sup>b\*</sup>

<sup>a</sup> Department of Physics and Physical Oceanography, Memorial University of Newfoundland, St. John's, Newfoundland and Labrador, Canada A1B3X7. E-mail: [lbeaulieu@mun.ca](mailto:lbeaulieu@mun.ca)

<sup>b</sup> Department of Chemistry, Memorial University of Newfoundland, St. John's, Newfoundland and Labrador, Canada A1B3X7. E-mail: [parisg@mun.ca](mailto:parisg@mun.ca)

<b>Table of Contents</b>	<b>Page</b>
<u>Computational study</u>	S2
Table S1 Selected parameter distances for <b>2</b> complex with Hg <sup>2+</sup>	S2
Figure SI 1. Binding mode of host calix[4]arene-triazole <b>2</b> with Hg <sup>2+</sup> ion.	S3
Figure SI 2: Ellipsoid structures of <b>2</b> and <b>2</b> ⊃Hg <sup>2+</sup> complex	S3
Figure SI 3: Ball-and-stick structures of <b>2</b> and <b>2</b> ⊃Hg <sup>2+</sup> complex	S4
Figure SI 4: Spacefill structures of <b>2</b> and <b>2</b> ⊃Hg <sup>2+</sup> complex	S4
Figure SI 5: Fluorescence spectra of <b>2</b> upon addition of Cd <sup>2+</sup> and binding model for <b>2</b> with Cd <sup>2+</sup>	S5
Figure SI 6: Fluorescence spectra of <b>2</b> upon addition of Cd <sup>2+</sup> and binding model for <b>2</b> with Co <sup>+</sup>	S5
Figure SI 7: Fluorescence spectra of <b>2</b> upon addition of Pb <sup>2+</sup> and binding model for <b>2</b> with Pb <sup>2+</sup>	S5
Figure SI 8: Fluorescence spectra of <b>2</b> upon addition of Zn <sup>2+</sup> and binding model for <b>2</b> with Zn <sup>2+</sup>	S6
Figure SI 9: Fluorescence spectra of <b>2</b> upon addition of Cu <sup>2+</sup> and binding model for <b>2</b> with Cu <sup>2+</sup>	S6
Figure SI 10: Fluorescence spectra of <b>2</b> upon addition of Fe <sup>2+</sup> and binding model for <b>2</b> with Fe <sup>2+</sup>	S7
Figure SI 11: Fluorescence spectra of <b>2</b> upon addition of Ni <sup>2+</sup> and binding model for <b>2</b> with Ni <sup>2+</sup>	S7
Figure SI 12: Metal competitive fluorescence quenching titration spectra of <b>2</b> with Hg <sup>2+</sup> in presence of various metals ions (M <sup>n+</sup> ).	S8
Figure SI 13: <sup>1</sup> H NMR, and <sup>13</sup> C-NMR spectrum of compound <b>2</b>	S9
Figure SI 14: <sup>1</sup> H NMR, and <sup>13</sup> C-NMR spectrum of compound <b>4</b>	S10
Figure SI 15: MS spectrum of compound <b>4</b>	S11
Figure SI 16: APPI HRMS spectrum of compound <b>2</b>	S12
Figure SI 17: MALDI-TOF spectrum of <b>2</b> with dithranol matrix.	S13
Figure SI 18: MALDI-TOF spectrum of <b>2</b> +Pb(ClO <sub>4</sub> ) <sub>2</sub>	S14
Figure SI 19: HRMS spectrum of complex <b>2</b> with Hg <sup>2+</sup>	S15
Figure SI 20: HRMS spectrum of complex <b>2</b> with Fe <sup>3+</sup>	S16
References	S17

## DFT Calculations:

The geometries of the molecular structures were optimized with either the B3LYP or PBE0 functionals with the LANL2DZ basis set. The DFT level of theory using the hybrid Perdew-Burke-Ernzerhof parameter free-exchange correlation functional PBE0 (PBE1PBE in the Gaussian realization)<sup>1</sup> with the Hay and Wadt effective core potential LANL2DZ basis set<sup>2</sup>. The starting structure was generated using *SpartanPro10* with the MMFF94 method.<sup>3</sup> The generated structures were then imported into *Gaussian-09 Revision D.01*<sup>4</sup> and were geometry-optimized in the gas-phase with either the B3LYP or PBE0 functionals with the LANL2DZ basis set. The N--N distance between the triazole ring nitrogens decreases from 5.795 Å to 3.609 Å and 6.221 Å to 3.743 (Å) since the nitrogen atoms moved in towards each other after **2** complexes with Hg<sup>2+</sup> (as shown in Fig. 1). The H--H distance between the triazole ring hydrogen increases from 6.079 Å to 9.918 Å, due to the hydrogen atoms moving away from each other. A <sup>1</sup>H NMR titration complexation study shows that the triazole ring hydrogen peak shifts downfield (+Δδ= 0.45 ppm) after complexing with Hg<sup>2+</sup> in solution. This is in agreement with the computational result that shows that the H--H distance between the triazole ring hydrogen increases from 6.076 Å to 9.918 Å. The calculated binding or interaction energies (IE) are -1426.8 kJ/mole using PBE0/LANL2DZ and -1385.03 KJ/mole using B3LYP with LANL2DZ basis set.

The binding energies (IE) of the complex were calculated according to equation (1):

$$IE = E_{\text{Complex}} - \Sigma(E_{\text{Calixtriazole}} + E_{\text{Hg}^{2+} \text{ ion}}) \quad (1)$$

**Table 1** The distances (Å) for the selected backbone atoms of the calix[4]arene-triazole-**2** and its complex with Hg<sup>2+</sup> ion optimized at PBE0/lanl2dz basis set in the gas phase at 298 K.

Distance (Å)	N <sub>5</sub> -N <sub>12</sub>	N <sub>6</sub> -N <sub>13</sub>	H <sub>116</sub> -H <sub>183</sub>	Hg <sup>2+</sup> -N <sub>6</sub>	Hg <sup>2+</sup> -N <sub>13</sub>	Hg <sup>2+</sup> -O <sub>41</sub>	Hg <sup>2+</sup> -O <sub>58</sub>
<b>B3LYP/lanl2dz</b>							
<b>Free host 2</b>	6.207	5.557	6.056	-	-	-	-
<b>2⊃Hg<sup>2+</sup></b>	3.643	3.782	10.078	2.322	2.323	2.403	2.424
<b>PBE0/lanl2dz</b>							
<b>Free host 2</b>	5.795	6.221	6.056	-	-	-	-
<b>2⊃Hg<sup>2+</sup></b>	3.609	3.743	9.918	2.309	2.299	2.471	2.367

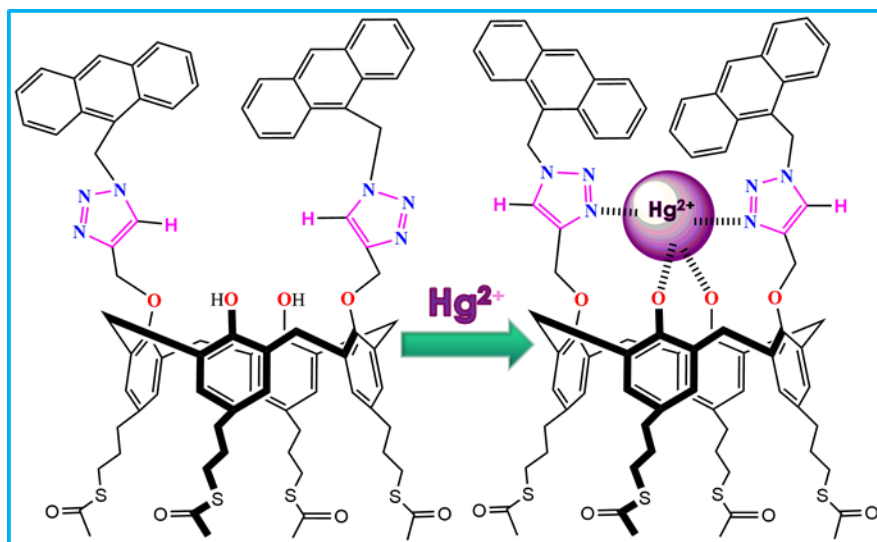


**Figure SI 1.** Binding mode of host calix[4]arene-triazole **2** with  $\text{Hg}^{2+}$  ion.

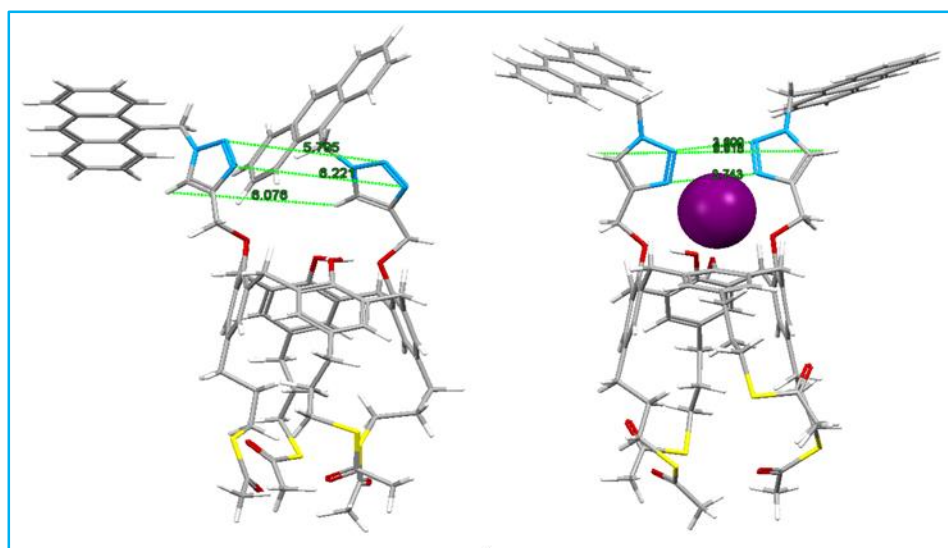


**Figure SI 2.** Geometry-optimized (PBE0/LANL2DZ) structures of **2** with complex  $\text{Hg}^{2+}$  ion. *Left:* The free host calix[4]arene-triazole **2** (Ellipsoid); *Right:* Calix[4]aren-triazole **2** complex with  $\text{Hg}^{2+}$  ion (Ellipsoid). Colour code: carbon = drack grey and oxygen atom = red, nitrogen = blue, sulphur = yellow and  $\text{Hg}^{2+}$  = purple.

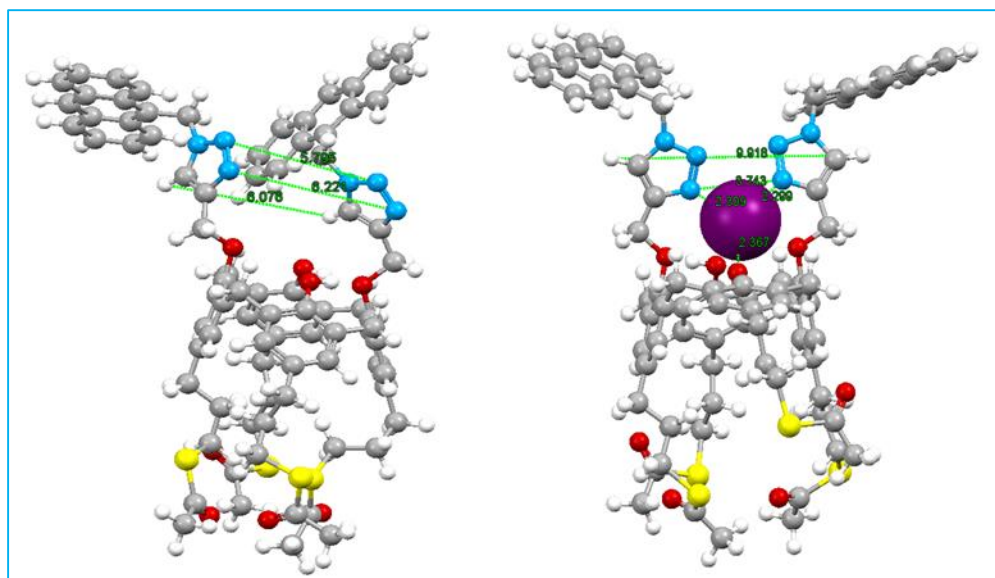


**Figure SI 3.** Geometry-optimized (PBE0/LANL2DZ) structures of **2** with complex  $\text{Hg}^{2+}$  ion. *Left:* The free host calix[4]arene-triazole **2** (Ball-and -stick); *Right:* Calix[4]arene-triazole **2** complex with  $\text{Hg}^{2+}$  ion (Ellipsoid). Colour code: carbon = drack grey and oxygen atom = red, nitrogen = blue, sulphur = yellow and  $\text{Hg}^{2+}$  = purple.

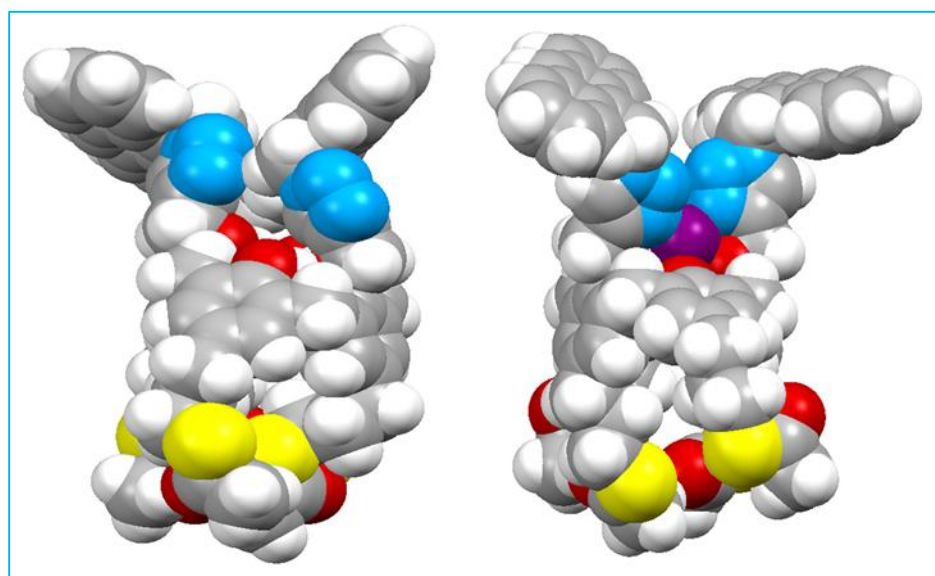


**Figure SI 4.** Geometry-optimized (PBE0/LANL2DZ) structures of **2** with complex  $\text{Hg}^{2+}$  ion. *Left:* The free host calix[4]arene-triazole **2** (Spacefill); *Right:* Calix[4]arene-triazole **2** complex with  $\text{Hg}^{2+}$  ion (Ellipsoid). Colour code: carbon = drack grey and oxygen atom = red, nitrogen = blue, sulphur = yellow and  $\text{Hg}^{2+}$  = purple.

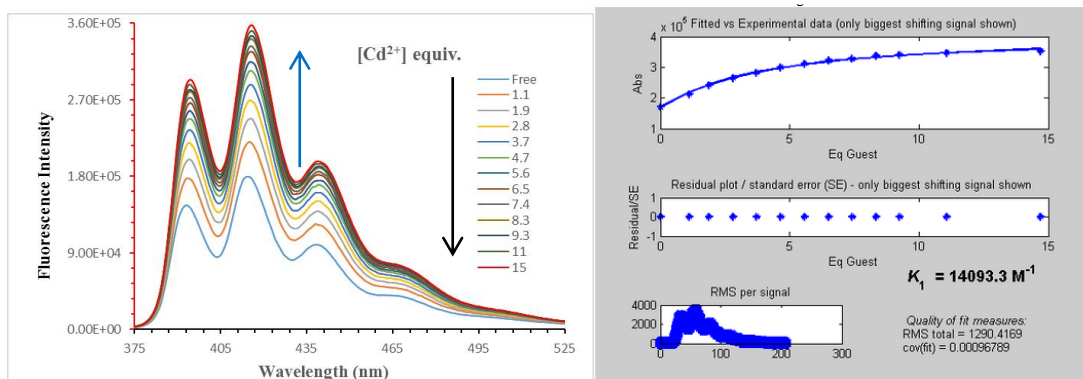


**Figure SI 5:** *Left:* Fluorescence spectra of **2** upon addition of Cd<sup>2+</sup> (1.1 to 15 eq) in acetonitrile/ chloroform (v/v= 9:1) solutions.  $\lambda_{ex}$  = 350 nm. *Right:* Screen-capture output showing 1:1 binding model for **2** with Cd<sup>2+</sup>, using Thordarson's<sup>5</sup> method.

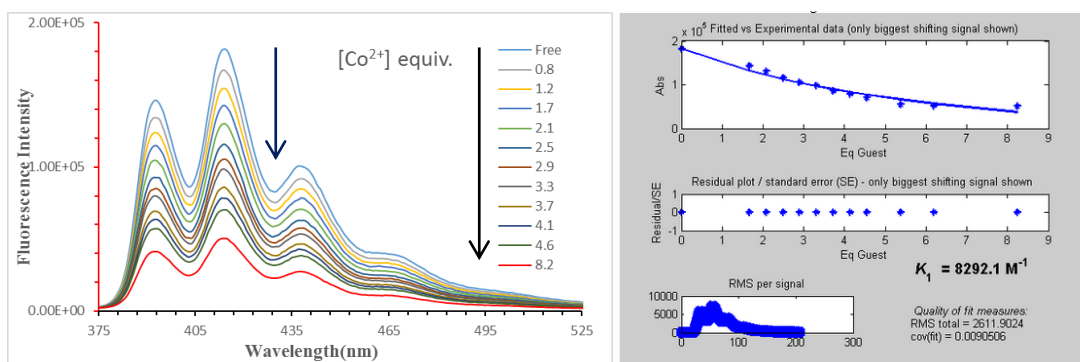


**Figure SI 6:** *Left:* Fluorescence spectra of **2** upon addition of Co<sup>2+</sup> (0.8 to 8.2 eq) in acetonitrile/ chloroform (v/v= 9:1) solutions.  $\lambda_{ex}$  = 350 nm. *Right:* Screen-capture output showing 1:1 binding model for **2** with Co<sup>2+</sup>, using Thordarson's<sup>5</sup> method.

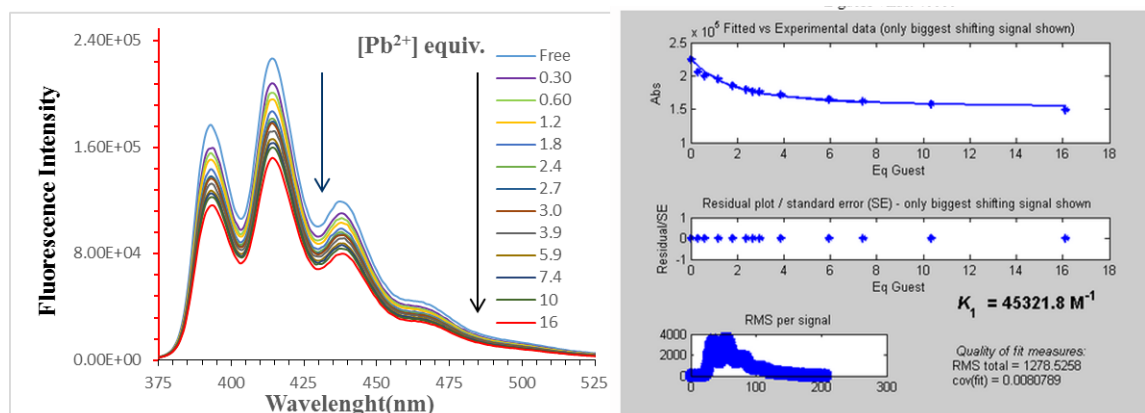


**Figure SI 7:** *Left:* Fluorescence spectra of **2** upon addition of Pb<sup>2+</sup> (0.30 to 16 eq) in acetonitrile/ chloroform (v/v= 9:1) solutions.  $\lambda_{ex}$  = 350 nm. *Right:* Screen-capture output showing 1:1 binding model for **2** with Pb<sup>2+</sup>, using Thordarson's<sup>5</sup> method.

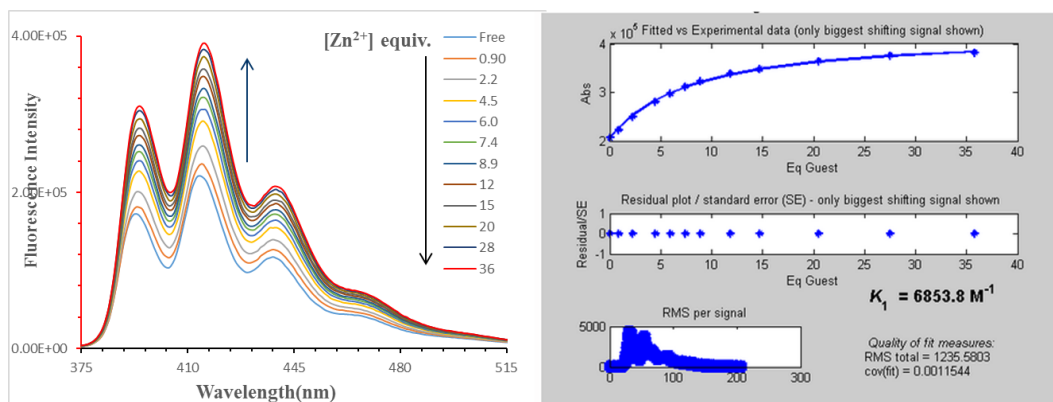


**Figure SI 8:** *Left:* Fluorescence spectra of **2** upon addition of Zn<sup>2+</sup> (0.90 to 36 eq) in acetonitrile/ chloroform (v/v = 9:1) solutions.  $\lambda_{ex} = 350 \text{ nm}$ . *Right:* Screen-capture output showing 1:1 binding model for **2** with Zn<sup>2+</sup>, using Thordarson's<sup>5</sup> method.

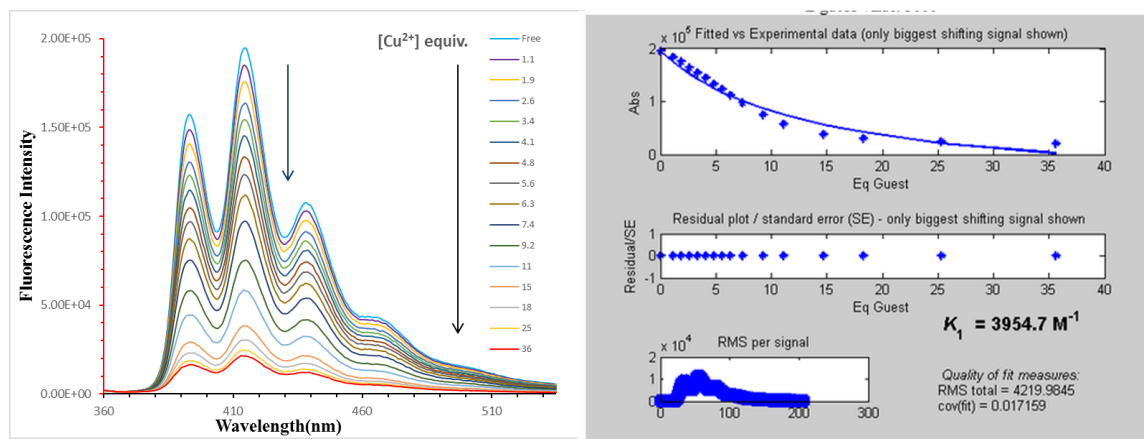


**Figure SI 9:** *Left:* Fluorescence spectra of **2** upon addition of Cu<sup>2+</sup> (1.1 to 36 eq) in acetonitrile/ chloroform (v/v = 9:1) solutions.  $\lambda_{ex} = 350 \text{ nm}$ . *Right:* Screen-capture output showing 1:1 binding model for **2** with Cu<sup>2+</sup>, using Thordarson's<sup>5</sup> method.

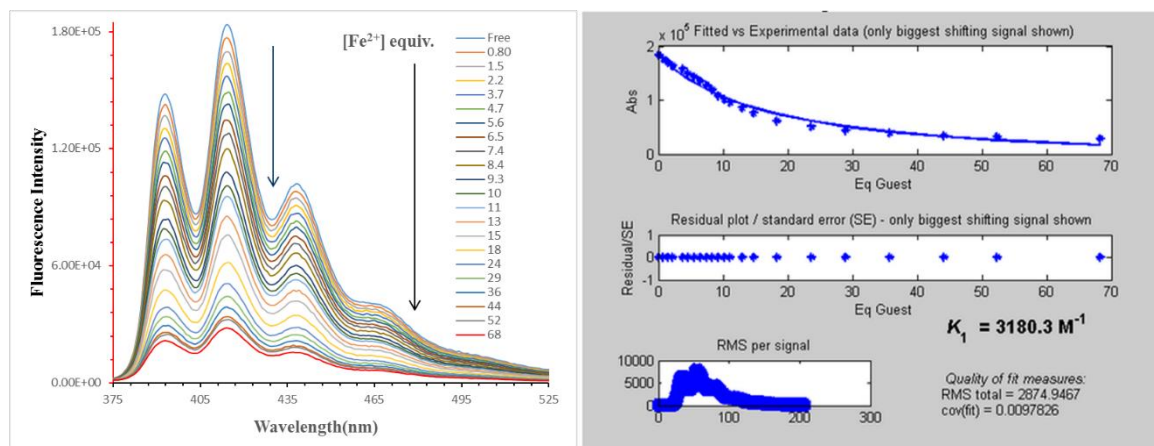


**Figure SI 10:** *Left:* Fluorescence spectra of **2** upon addition of Fe<sup>2+</sup> (0.80t to 68 eq) in acetonitrile/ chloroform (v/v= 9:1) solutions.  $\lambda_{ex} = 350 \text{ nm}$ . *Right:* Screen-capture output showing 1:1 binding model for **2** with Fe<sup>2+</sup>, using Thordarson's<sup>5</sup> method.

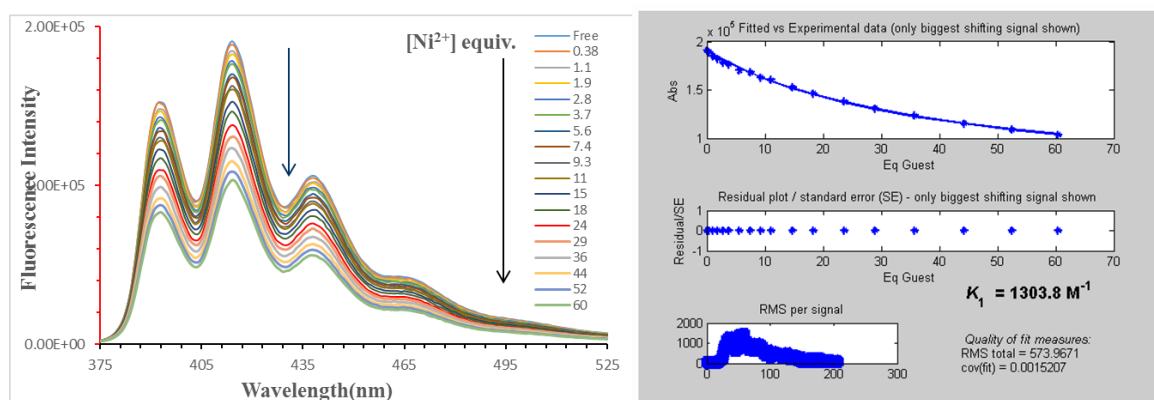


**Figure SI 11:** *Left:* Fluorescence spectra of **2** upon addition of Ni<sup>2+</sup> (0.38 to 60 eq) in acetonitrile/ chloroform (v/v= 9:1) solutions.  $\lambda_{ex} = 350 \text{ nm}$ . *Right:* Screen-capture output showing 1:1 binding model for **2** with Ni<sup>2+</sup>, using Thordarson's<sup>5</sup> method.



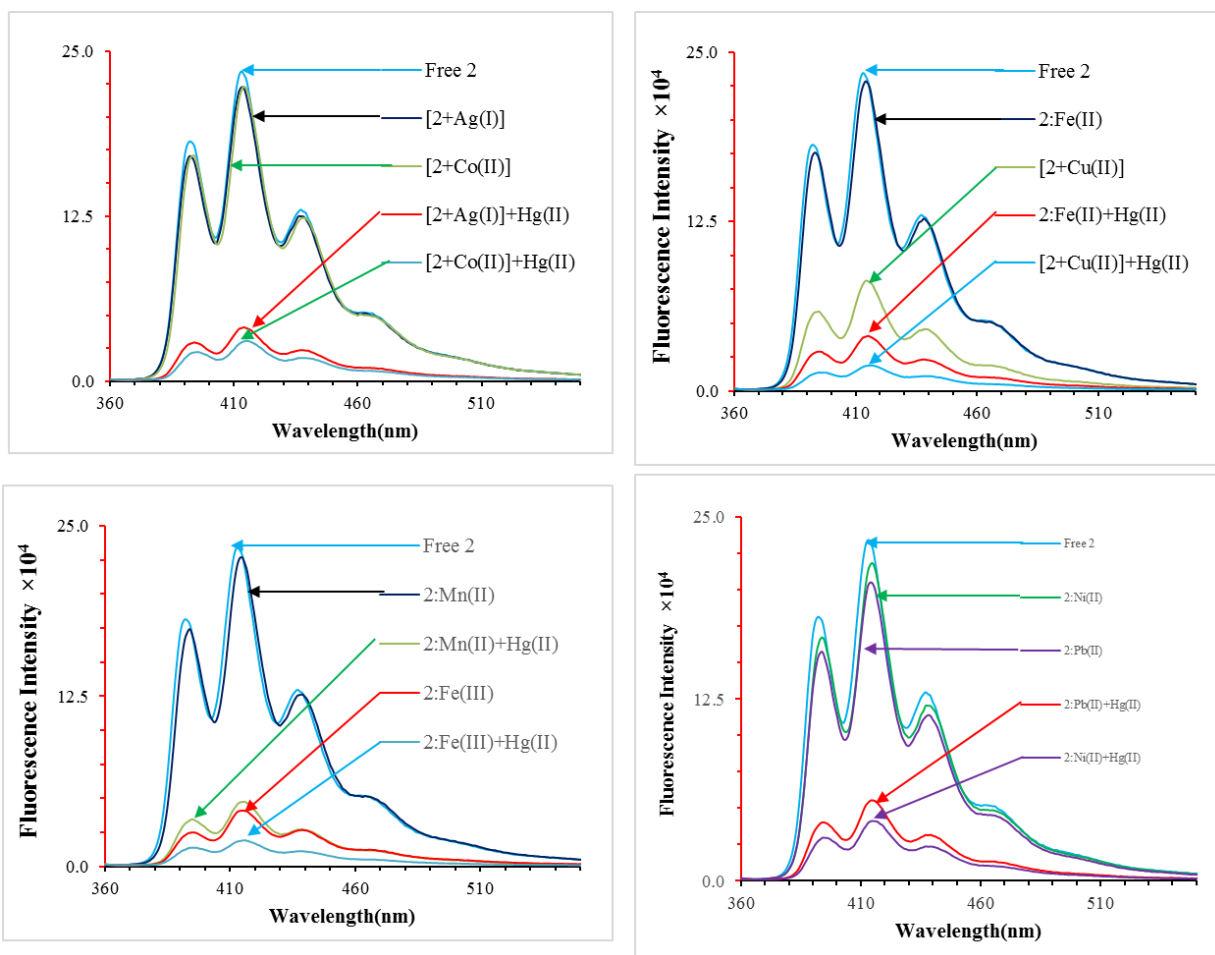


**Figure SI 12:** Metal competitive fluorescence quenching for the solutions of 1:1  $2:M^{n+}$  to which equimolar amounts of  $Hg^{2+}$  were added in  $CH_3CN:CHCl_3$  (9:1).



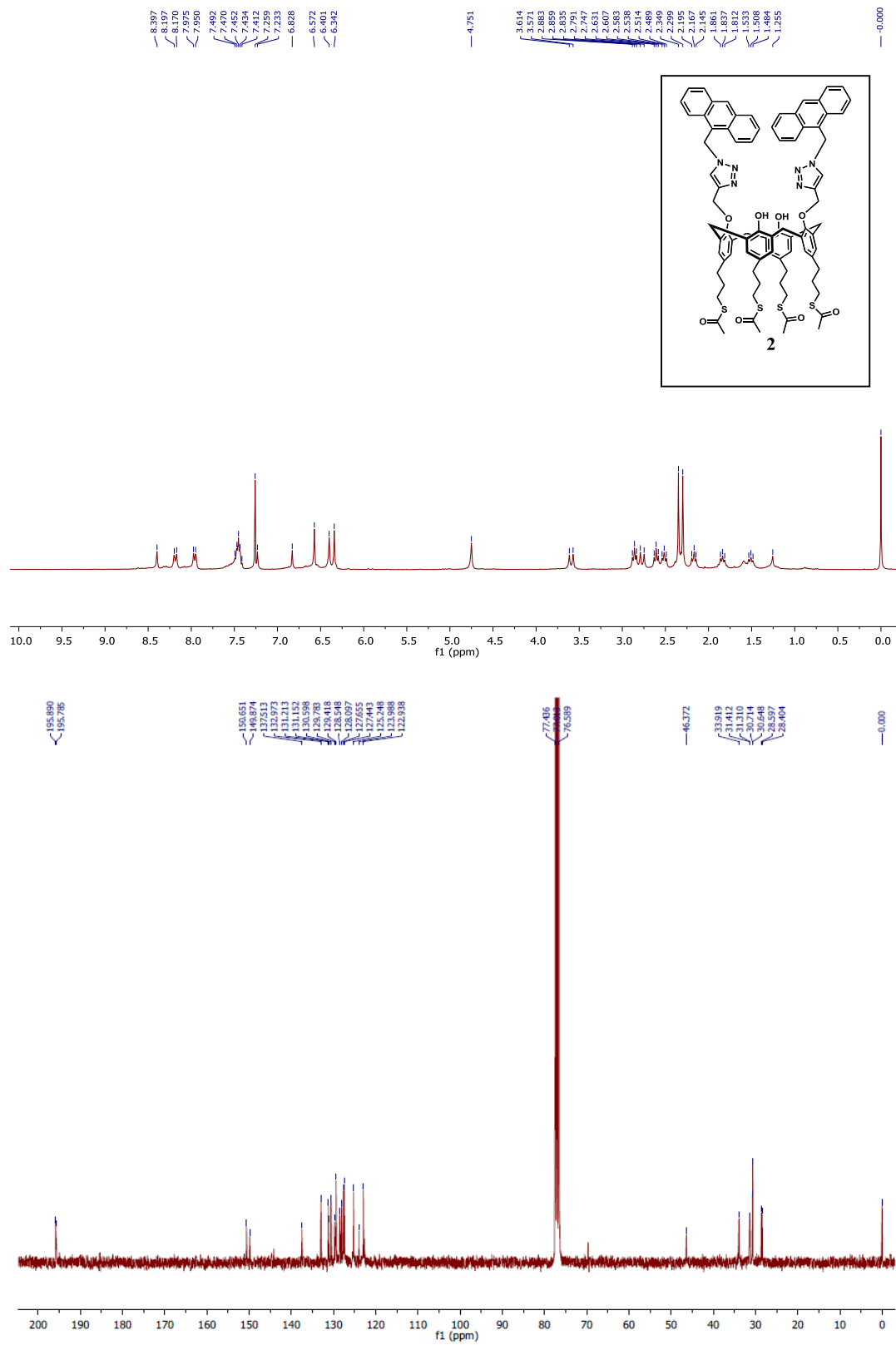
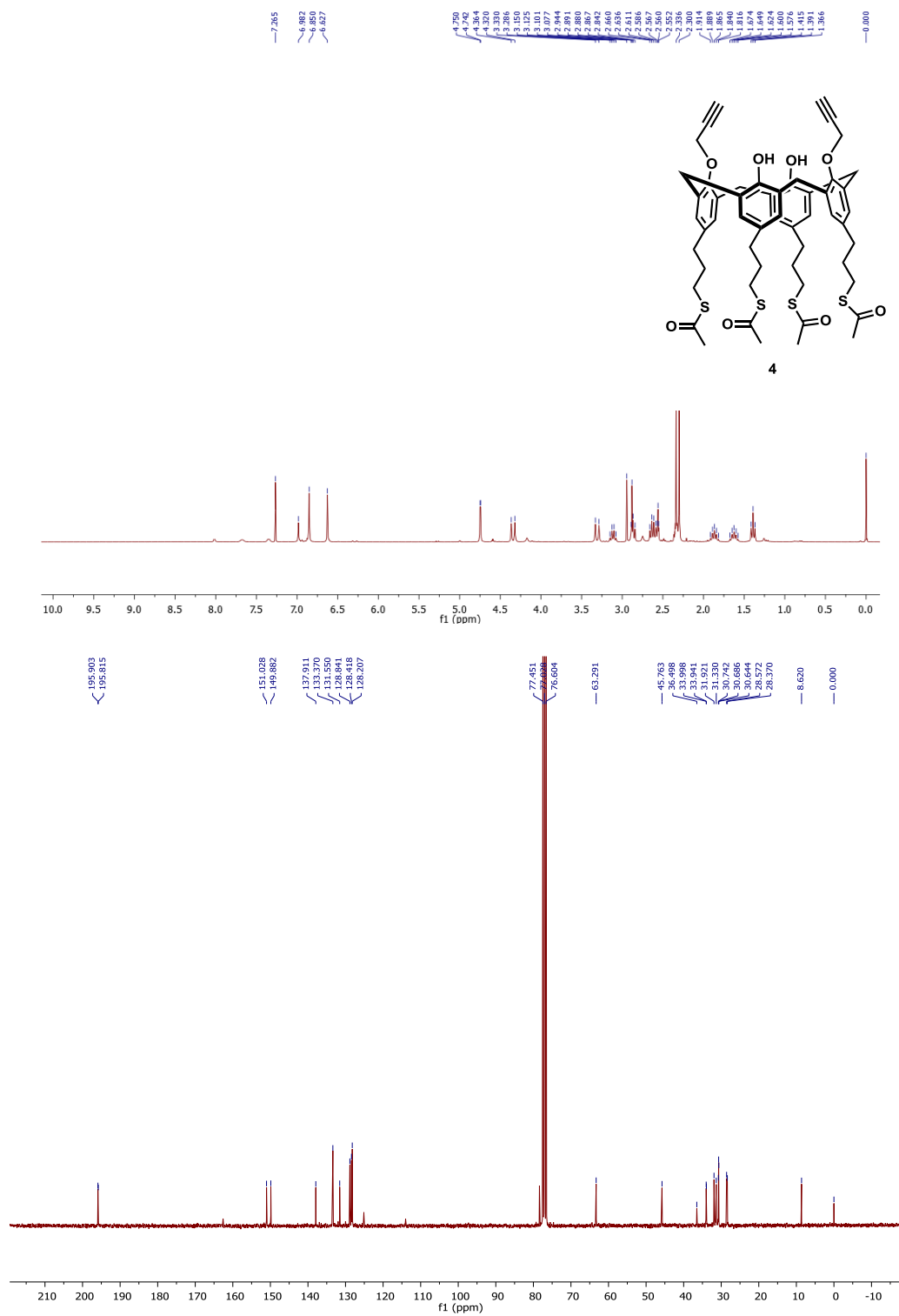
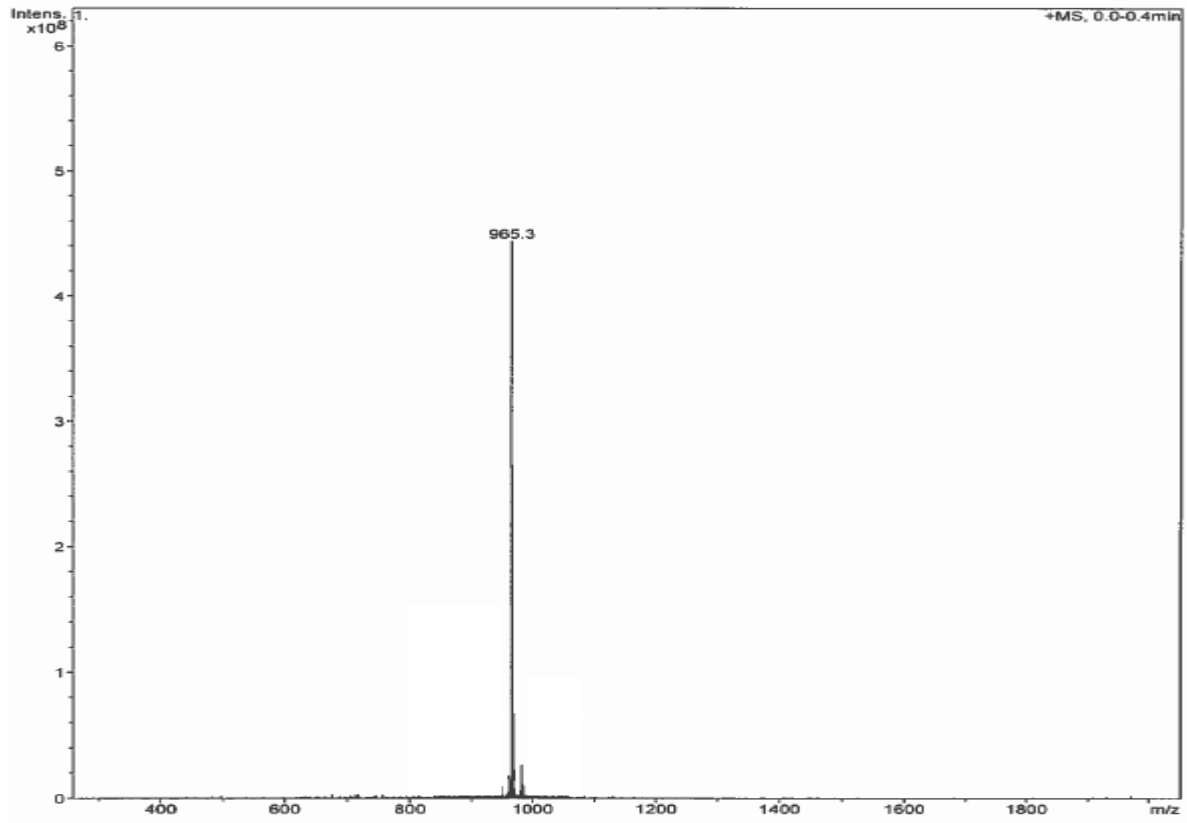


Figure SI 13: <sup>1</sup>H NMR, and <sup>13</sup>C-NMR spectrum of compound 2



**Figure SI 14:**  $^1\text{H}$  NMR, and  $^{13}\text{C}$ -NMR spectrum of compound **4**



**Figure SI 15:** MS spectrum of compound **4**

## Qualitative Compound Report

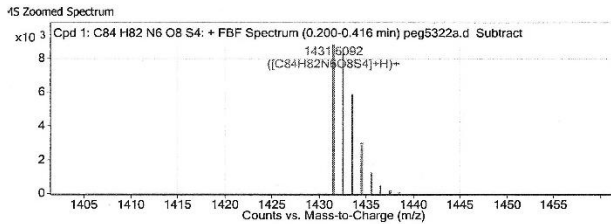
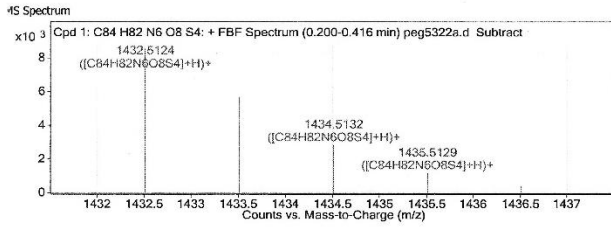
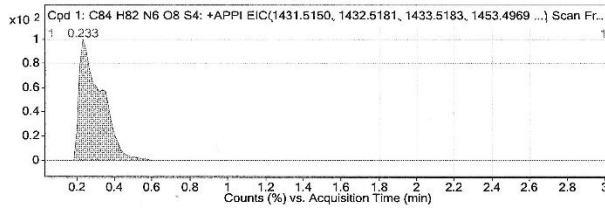
Data File	peg5322a.d	Sample Name	PG/GK #1
Sample Type	Sample	Position	Vial 1
Instrument Name	LCMS 1260_6230	User Name	crit-TOF\agilent
Acq Method	pgeorghiou.m	Acquired Time	10/13/2015 3:34:42 PM
IRM Calibration Status	Success	DA Method	gabualsoud.m
Comment	neat		

Sample Group Info.  
 Acquisition SW 6200 series TOF/6500 series  
 Version Q-TOF B.05.01 (B5125.3)

### Compound Table

Compound Label	RT	Mass	Abund	Formula	Tgt Mass	Diff (ppm)	MFG Formula	DB Formula
Cpd 1: C84 H82 N6 O8 S4	0.233	1430.502	8830	C84 H82 N6 O8 S4	1430.5077	-3.97	C84 H82 N6 O8 S4	C84 H82 N6 O8 S4

Compound Label	m/z	RT	Algorithm	Mass
Cpd 1: C84 H82 N6 O8 S4	1431.5092	0.233	Find By Formula	1430.502



### MS Spectrum Peak List

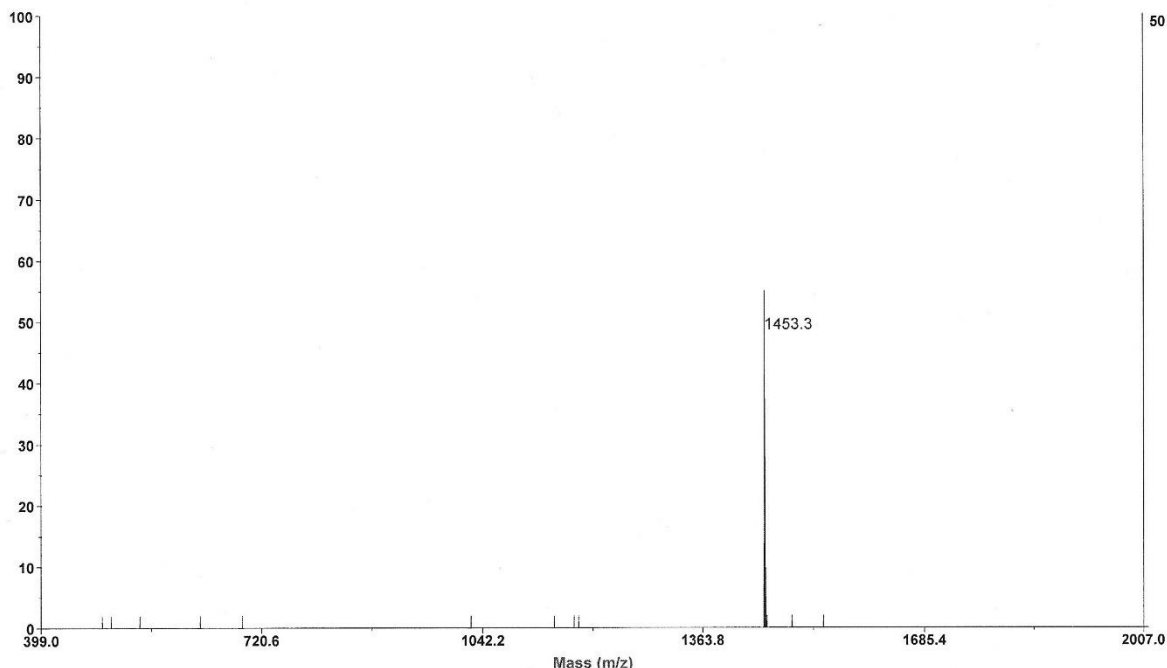
m/z	z	Abund	Formula	Ion
1431.5092	1	8830	C84H82N6O8S4	(M+H)+
1432.5124	1	8617.29	C84H82N6O8S4	(M+H)+
1433.5128	1	5699.72	C84H82N6O8S4	(M+H)+
1434.5132	1	2859.2	C84H82N6O8S4	(M+H)+
1435.5129	1	1180.96	C84H82N6O8S4	(M+H)+
1436.5151	1	413.24	C84H82N6O8S4	(M+H)+
1437.5131	1	80.81	C84H82N6O8S4	(M+H)+

--- End Of Report ---

**Figure SI 16:** APPI HRMS spectrum of compound 2

# Spectrum Report

Final - Shots 400 - AO5336; Label L3



## Summary

Serial Number 2003  
Instrument Name 4800 Instrument

## Spot

Plate Name peg  
Plate Barcode <<none>>  
Spot Set Name AO5336  
Job Run Comments <<none>>  
Spot Label L3  
Spot Name <<none>>  
Spot Type Unknown  
Location X Min 20571.807  
Location X Max 21579.583  
Location Y Min 26518.074  
Location Y Max 27594.172  
Spot Run # 1

Tallest Peak Height 2.391449e+001  
Tallest Peak S/N 14.3000  
Tallest Peak Mass 1453.2847  
Tallest Peak Resolution 20597.4180

## Calibration Coefficients

1.270039e+002  
3.781564e-007  
2.389361e-006

## Interpretation

Interpretation Method Name <<none>>

## Pressures

Source 2 2.4e-008 torr  
TC Turbo 7.7e-003 torr  
Source 1 1.5e-007 torr

## Spectrum

Rejected Sub-spectra 0  
Mass Acc. Opt. Cal Types Updated None  
Rejected Shots 0  
Update Default Calibration Disabled  
Stop Reason Unknown Error  
Total Accumulations 16  
Total Ion Count 1.900000e+002  
Total Shots 400  
Job-Wide Interpretation Disabled  
Configured for LCMS Experiments Disabled

## Acquisition

Method Name Reflector  
Mass Analysis Type MS Reflector Positive Ion Mode  
CID Off  
CID Gas Type Air  
CID Gas Pressure Medium  
Start Time 10/26/15 14:27:22  
Laser Intensity Range 4720 To 4720

## Processing

Processing Method Name reflector method  
Calibration Type Default  
Peak Count 1

Figure S17: MALDI-TOF spectrum of 2 with dithranol matrix.

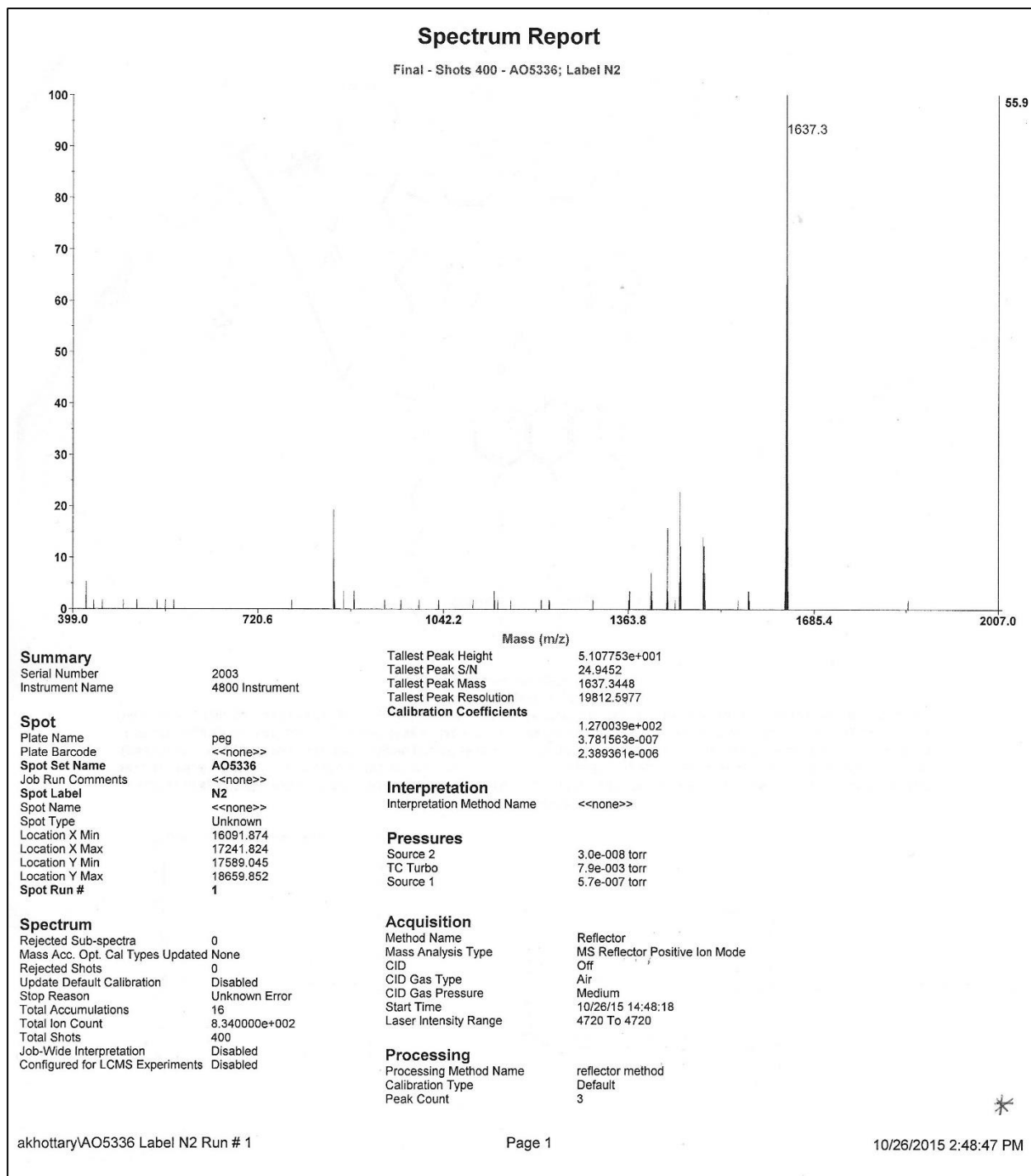
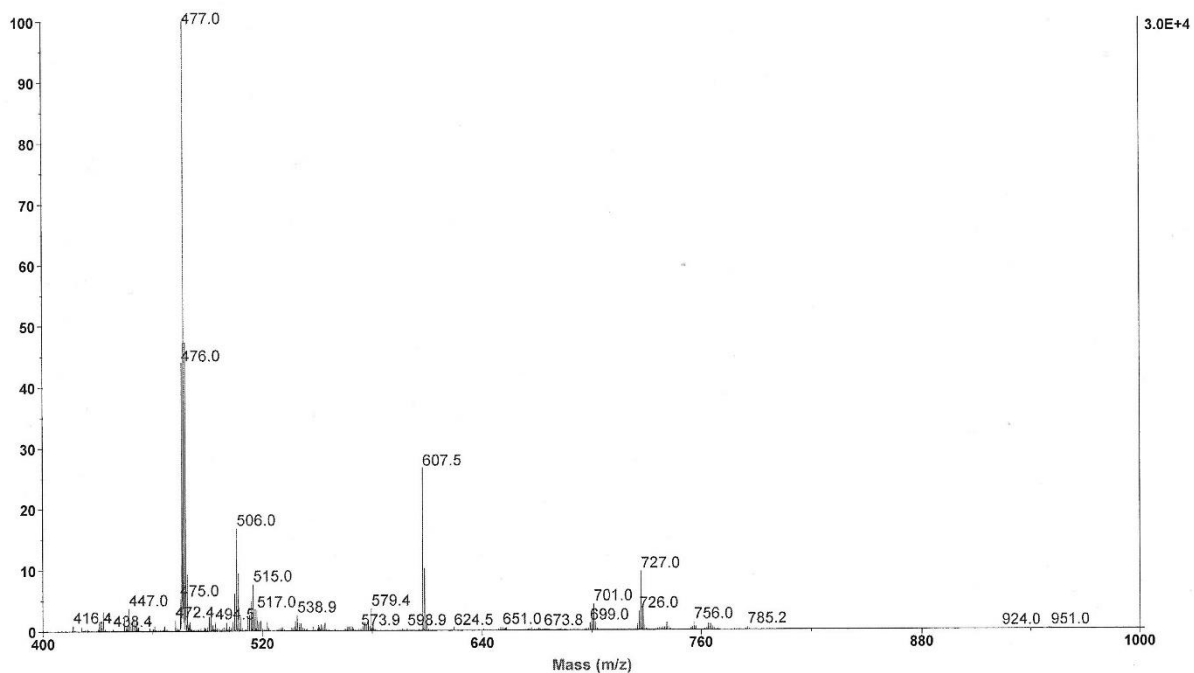


**Figure SI 18:** MALDI-TOF spectrum of 2+ Pb(ClO<sub>4</sub>)<sub>2</sub>.

# Spectrum Report

Final - Shots 400 - AO5337; Label D10



### Summary

Serial Number 2003  
Instrument Name 4800 Instrument

Tallest Peak Height 2.954755e+004  
Tallest Peak S/N 4893.9581  
Tallest Peak Mass 476.9815  
Tallest Peak Resolution 3687.9966

### Spot

Plate Name peg  
Plate Barcode <<none>>  
Spot Set Name AO5337  
Job Run Comments <<none>>  
Spot Label D10  
Spot Name <<none>>  
Spot Type Unknown  
Location X Min 52291.351  
Location X Max 52999.479  
Location Y Min 62605.387  
Location Y Max 63287.451  
Spot Run # 1

Calibration Coefficients  
1.270039e+002  
3.781664e-007  
2.389361e-006

### Interpretation

Interpretation Method Name <<none>>

### Pressures

Source 2 2.3e-008 torr  
TC Turbo 7.7e-003 torr  
Source 1 1.5e-007 torr

### Spectrum

Rejected Sub-spectra 0  
Mass Acc. Opt. Cal Types Updated None  
Rejected Shots 0  
Update Default Calibration Disabled  
Stop Reason Unknown Error  
Total Accumulations 16  
Total Ion Count 1.319434e+006  
Total Shots 400  
Job-Wide Interpretation Disabled  
Configured for LCMS Experiments Disabled

### Acquisition

Method Name Reflector  
Mass Analysis Type MS Reflector Positive Ion Mode  
CID Off  
CID Gas Type Air  
CID Gas Pressure Medium  
Start Time 10/27/15 14:06:16  
Laser Intensity Range 4870 To 4870

### Processing

Processing Method Name reflector method  
Calibration Type Default  
Peak Count 174

**Figure SI 19:** MALDI-TOF spectrum of  $\text{Hg}(\text{ClO}_4)_2$ .



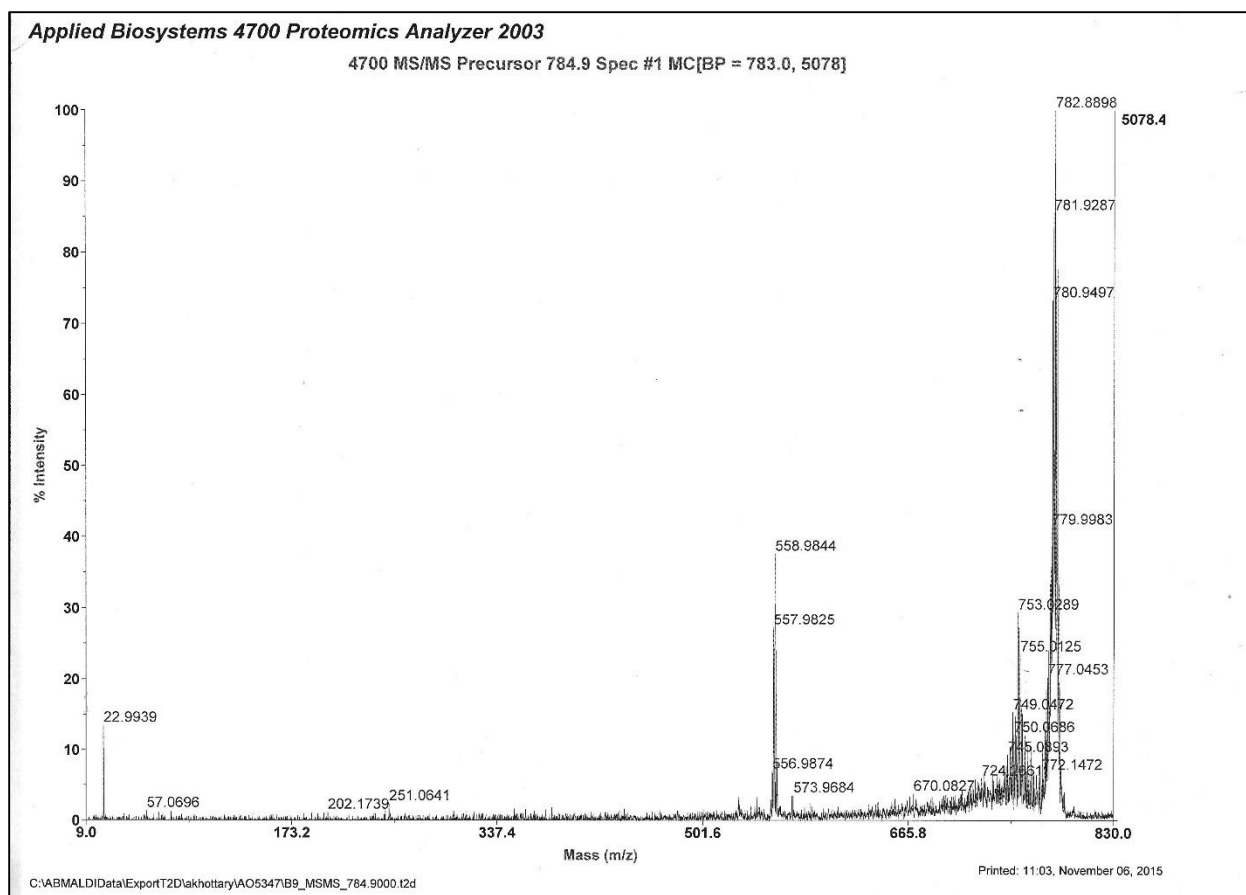


**Figure SI 20:** MALDI-TOF spectrum of complex **2** with  $\text{Fe}(\text{ClO}_4)_3$ .

References:

1. (a) Perdew, J. P.; Burke, K.; Ernzerhof, M. *Phys. Rev. Lett.* **1996**, *77*, 3865; (b) Perdew, J. P.; Burke, K.; Ernzerhof, M. *Phys. Rev. Lett.*, **1997**, *78*, 1396.
2. (a) Hay, P. J.; Wadt, W. R. *J. Chem. Phys.*, **1985**, *82*, 270; (b) Hay, P. J.; Wadt, W. R. *J. Chem. Phys.* **1985**, *82*, 284; (c) Hay, P. J.; Wadt, W. R. *J. Chem. Phys.* **1985**, *82*, 299.
3. Initial molecular modeling calculations using the MMFF94 method were performed using the *PC Spartan'10* software from Wavefunction Inc., Irvine CA.M.
4. Frisch, M. J.; Trucks, G. W.; Schlegel, H. B.; Scuseria, G. E.; Robb, M. A.; Cheeseman, J. R.; Scalmani, G.; Barone, V.; Mennucci, B.; Petersson, G. A.; Nakatsuji, H.; Caricato, M.; Li, X.; Hratchian, H. P.; Izmaylov, A. F.; Bloino, J.; Zheng, G.; Sonnenberg, J. L.; Hada, M.; Ehara, M.; Toyota, K.; Fukuda, R.; Hasegawa, J.; Ishida, M.; Nakajima, T.; Honda, Y.; Kitao, O.; Nakai, H.; Vreven, Jr., T.; Montgomery, J. A.; Peralta, J. E.; Ogliaro, F.; Bearpark, M.; Heyd, J. J.; Brothers,

E.; Kudin, K. N.; Staroverov, V. N.; Keith, T.; Kobayashi, R.; Normand, J.; Raghavachari, K.; Rendell, A.; Burant, J. C.; Iyengar, S. S.; Tomasi, J.; Cossi, M.; Rega, N.; Millam, J. M.; Klene, M.; Knox, J. E.; Cross, J. B.; Bakken, V.; Adamo, C.; Jaramillo, J.; Gomperts, R.; Stratmann, R. E.; Yazyev, O.; Austin, A. J.; Cammi, R.; Pomelli, C.; Ochterski, J. W.; Martin, R. L.; Morokuma, K.; Zakrzewski, V. G.; Voth, G. A.; Salvador, P.; Dannenberg, J. J.; Dapprich, S.; Daniels, A. D.; Farkas, O.; Foresman, J. B.; Ortiz, J. V.; Cioslowski, J.; Fox, D. J. Gaussian 09, Revision D.01; Gaussian, Inc., Wallingford CT, 2013.

5. (a) Thordarson, P. *Chem. Soc. Rev.* **2011**, *40*, 1305-1323. (b) <http://supramolecular.org>